Journal of Catalysis **187,** 39–49 (1999)
Article ID jcat.1999.2573, available online at http://www.idealibrary.com on IDEAL®

Coking of SO_4^{2-}–ZrO_2 Catalysts during Isomerization of *n*-Butane and Its Relation to the Reaction Mechanism

Carlos R. Vera,*[,1] Carlos L. Pieck,†[,2] Kiyoyuki Shimizu,*[,3] Carlos A. Querini,† and J. M. Parera†

**National Institute for Resources and Environment—NIRE—(AIST, MITI), 16-3 Onogawa, Tsukuba 305-8569, Japan; and †Instituto de Investigaciones en Catálisis y Petroquímica—INCAPE—(FIQ-UNL, CONICET), Santiago del Estero 2654, 3000 Santa Fe, Argentina*

Received December 3, 1998; revised May 17, 1999; accepted May 24, 1999

A study of the deactivation of SO_4^{2-}–ZrO_2 catalysts during isomerization of *n*-butane showed that a small amount of a carbonaceous deposit (1–1.2%) is formed. A high proportion of this deposit is produced during the first minutes of the reaction and it seems to be responsible for the initial short-term catalyst deactivation but it is doubtful whether it is connected to the long-term loss of activity. Activity in isomerization of *n*-C_4 was very sensitive to activation conditions while coking was more consistent; in all cases, SZ catalysts had a limiting content of 1 to 1.2% coke when fully deactivated. In an oxygen flow, the coke deposit could be burned at 500°C, but it could also easily be removed by stripping with an oxygen-free inert gas at higher temperatures. In the latter case, the coke was oxidized by the catalyst surface groups, most likely sulfate. The coke was soluble only in polar solvents (methanol, pyridine) and was highly insoluble in benzene and hexane. An FD-mass spectrum of the soluble fraction of the coke indicated the presence of compounds with m/z up to 2700, but the distribution was concentrated around $m/z = 350$ to 500. The latter value, when compared with the small amount of total carbon, indicates that only a small fraction of the surface sites was affected by the coke, or that deactivation proceeded by a mechanism other than site blocking. A surface reduction process by the reacting hydrocarbon may also be linked to the activity loss. ESR results indicated that the catalyst was also reduced during the reaction; the intensity of the Zr^{3+} signal was higher on the coked catalysts. The probable concurrence of reduction could explain the long-term activity decline which seems not to be directly linked to the coking process.

Key Words: **coking; sulfated zirconia; *n*-butane isomerization.**

INTRODUCTION

SO_4^{2-}–ZrO_2 (SZ) catalysts display high activity and selectivity in the isomerization of light paraffins, being also important experimental catalysts for several processes of interest such as hydrocracking, alkylation, and acylation (1, 2). Their big drawback, which hampers their industrial application, is their fast deactivation following contact with hydrocarbons (3). Some authors (4, 5) suggested that deactivation is due to a reduction in the oxidation state of sulfur. Such reduction may proceed until sulfur species are removed from the surface of the catalyst. Sulfur losses have indeed been detected both in the activation step at high temperatures and during the reaction (6). Ng and Horvat (7) detected sulfur species in exhaust gases during the isomerization of *n*-butane. SO_2 is more likely to be released, according to a recent study on the reduction of SZ (8). Sulfur reduction through formation of sulfite species has also been suggested (9, 10). Sulfur losses are likely to be due to highly labile sulfate groups. They do not produce an irreversible deactivation; regeneration with air at high temperatures results in the recovery of the initial level of conversion (6). The sulfur removed may correspond to a small fraction of sites that do not contribute significantly to the total activity. Yori and Parera (11) demonstrated that only a small fraction of total sulfate is necessary for the maintenance of much of the total activity of Pt/SO_4^{2-}–ZrO_2 catalysts.

At present, most authors believe that the coke formation is the cause of deactivation (12, 13). Water, too, acts as a deactivating poison, an effect shown by the elimination of Lewis acid sites thought to be involved in the *n*-C_4 isomerization mechanism (6, 14). It seems clear that in order to be applied industrially, the life cycle of SO_4^{2-}–ZrO_2 catalysts should be at least similar to that of naphta reforming, so that a simple and low-cost technology of regeneration can be applied. The research efforts in this area have been aimed at the preparation of Pt/SO_4^{2-}–ZrO_2; the metal function in the presence of hydrogen would provide atomic hydrogen for the removal of coke precursors. Some encouraging results were presented at first (15). However, the Pt cannot be completely reduced to the metallic state (16, 17) and very high hydrogen partial pressures are needed to stabilize the catalyst (18, 19). In any case, a better knowledge of the deactivation process is needed in order to devise suitable measures to counteract it.

---

[1] Guest researcher at NIRE during 1998, permanent affiliation to INCAPE; currently at the Institute Français du Pétrole (Vernaison, France).

[2] Currently at the Instituto de Catálisis y Petroleoquímica (Madrid, Spain).

[3] Currently at the Loker Hydrocarbon Research Institute, University of Southern California (Los Angeles, CA).

0021-9517/99 $30.00

In this work, we investigated some features of the coking process. An analysis of activity and selectivity and their relationship with the degree of deactivation during isomerization of *n*-butane was performed. A study of the relationship of the coke content with time-on-stream and the temperature of activation was also undertaken. The coke deposit was analyzed by TPO/TPD and FD-MS. Additional studies of clean and coked surfaces of SZ were performed by ESR to assess the presence of reduced species before and after reaction.

EXPERIMENTAL

Catalysts. $Zr(OH)_4$ (ZH) was prepared following a technique described elsewhere (20). It was sulfated by immersion in a 1 N solution of H_2SO_4 for 2 h and then washed, filtered, and dried in a stove at 110°C overnight (sample SZH). Precalcined sulfated zirconia (CSZ) was prepared by calcining portions of the SZH batch in air at 620°C for 3 h. Precalcination was aimed at stabilizing the sulfur level and obtaining the tetragonal active crystal phase.

Selectivity analysis. A compilation of experimental runs of *n*-butane isomerization was analyzed. They comprised reactions performed under different conditions ($\mathrm{WHSV} = 0.8$ to $2.5\ \mathrm{h}^{-1}$, activation in air at 620 to 720°C for 3 h) and using SO_4^{2-}–ZrO_2 catalysts prepared by sulfation of Zr hydroxide obtained from different precursors (*n*-butoxide (21), *n*-propoxide, chloride (22), and oxychloride (20)). Reaction temperature was 300°C and reaction times were 1 to 4 h.

Textural properties. The textural properties of the catalysts were determined in three states: (i) sulfated and uncalcined (SZH), (ii) sulfated and calcined at 620°C for 3 h (CSZ), (iii) coked after the reaction ($\mathrm{CSZ}^{\mathrm{coked}}$, in pure *n*-butane for 3 h, $\mathrm{WHSV} = 1.6\ \mathrm{h}^{-1}$). A Quantachrome NOVA-1000 sortometer was used for the measurements. SZH was degassed at 100°C *in vacuo* for 2 h before measurement. Calcined samples (CSZ and $\mathrm{CSZ}^{\mathrm{coked}}$) were degassed 1 h at 200°C. The 1-point BET method was used for surface measurement at a relative pressure of nitrogen of $p/p_o = 0.3$. The measurement of pore volume was performed by nitrogen adsorption at $p/p_o = 0.99$. The mean pore radius was determined by Wheeler's formula ($R_p = 2V_p/Sg$). The pore distribution was determined by the BJH method applied to the desorption isotherm (77.4 K) of N_2. X-ray diffraction was performed in Shimadzu XD-1 equipment. Radiation was $\mathrm{Cu}K\alpha$ filtered with Ni.

Coking studies. Different coked samples were characterized with the aid of temperature-programmed oxidation (TPO). The coke content and burning profile were determined as a function of time-on-stream, temperature of activation, and hydration state. Coking was performed using pure *n*-butane (Matheson, 99.99%+) both in continuous flow ($\mathrm{WHSV} = 2.5$ to $0.8\ \mathrm{h}^{-1}$) and in pulse mode.

The apparatus for the TPO tests consisted basically of three parts: (i) a cell containing the coked catalyst where the combustion of the carbonaceous deposit took place under a flow of oxygen diluted in an inert gas (6% in N_2); (ii) a methanator, a bed of Ni/Kieselguhr catalyst, where CO_2 was transformed quantitatively to CH_4 at $T = 400°\mathrm{C}$ under a hydrogen flow (30 $\mathrm{cm}^3\ \mathrm{min}^{-1}$); (iii) a flame ionization detector (FID, 22 ml min^{-1} H_2, 320 ml min^{-1} air) where the CH_4 produced in the methanator was monitored. Details of the technique have been reported by Fung and Querini (23). The heating rate of the combustion cell was 12°C min^{-1}.

In order to study the coking pattern during the first minutes of reaction and the impact of hydration on coking, CSZ hydrated samples (dipped in water for 30 min and then dried at 100°C) were activated in air at 620°C (1 h, CSZ^{620}, thoroughly dehydrated) and 300°C (30 min, CSZ^{300}, hydrated) before starting the reaction in pulse mode. Up to 700 ml of *n*-butane was injected and reacted.

For the study of the influence of activation temperature on the initial catalytic activity and the coke content, sulfated zirconium hydroxide (SZH) was used. Activation consisted of 2 h calcination in dry air (10 ml $\mathrm{min}^{-1}\ \mathrm{g}_{\mathrm{cat}}^{-1}$). WHSV was 2.5 h^{-1} (continuous flow regime) and the first measurement was performed at 5 min. Initial activity at 5 min and final coke content after 3 h were measured.

Catalytic test. Isomerization of *n*-butane performed both in the flow and pulse regimes was used. The pulse reaction system consisted basically of two elements: (i) a six-port valve used for the loading and injection of the pulses; and (ii) a quartz, 20-cm-long microreactor of small diameter (5 mm) where the reaction took place. The connections from and to the microreactor had a diameter of 1/16″ (1.587 mm) in order to minimize the distortion of the pulse. Depending on the frequency of the pulses, they were either sent directly to the chromatographic column or collected in a gas-tight ampoule and analyzed off-line (thus allowing a higher frequency of reacting pulses). In the pulse test, the mass of catalyst used was always 0.2 g, sieved to 35–80 meshes. The spatial velocity of *n*-butane in the pulse regime was imposed by the velocity of the carrier (10 ml min^{-1}). Some coke stripping was detected depending on the frequency of injection and this effect had to be studied in order to set the appropiate frequency. Both nitrogen and air were used in these preliminary tests to see any influence of the carrier in the coke elimination.

In the continuous-flow tests, the mass used was always 0.5 g (35–80 meshes) and pure n-C_4 was used with no dilution. Where not specified otherwise, the activation treatments were performed in flowing air (10 ml $\mathrm{min}^{-1}\ \mathrm{g}_{\mathrm{cat}}^{-1}$) for 2 h at 620°C. At this calcination temperature the catalyst displays maximum conversion of *n*-butane and high selectivity to *i*-butane (24).

Solvent extraction and coke characterization. Different solvents and different conditions were used to assess the solubility of the coke deposits. Benzene-methanol, a solvent commonly used in reforming catalysts (25), was used for a first trial, and extraction was performed at ambient temperature and under agitation in an ultrasonic bath (1 h). Pyridine extraction was performed by reflux heating at 70 to 80°C for 40 min. Extractions with methanol, hexane, and benzene were performed in a 200-ml capacity Soxhlet for 8 h. In all the experiments, about 0.5 to 1 g of coked catalyst was extracted with 100 ml of solvent. Coke extracts were subjected to analysis by FD-mass spectrometry. The pyridine-soluble extract was used because in this extract coke solubilization was thought to be almost complete. The solvent was first evaporated and the remaining solid was analyzed in the m/z range 100 to 3000.

ESR. Coked (after reaction with pure *n*-C_4, WHSV = 2.5 h^{-1}, continuous flow, 300°C, 3 h) and uncoked CSZ catalysts were analyzed after removal from the equipment. ESR measurements were performed in a JEOL spectrometer operating in band *X* (9.7 GHz) at the temperature of liquid nitrogen (77.4 K). Quartz cells were used for the activation treatments and for the measurements. The samples (0.5 g) were evacuated at 300°C before the measurement (residual pressure <1 m Torr).

RESULTS

Textural and crystal properties. Table 1 depicts the textural parameters of the catalyst at different stages in the process of activation and reaction. The results clearly indicate that the reduction of the available area and the total pore volume take place almost exclusively during the activation treatment at temperatures near 620°C and are thought to be linked to the crystallization of the ZrO_2 support, a process of high ionic mobility that enhances the sintering. The changes occurring during the reaction did not affect the textural properties. Therefore, the coking of SO_4^{2-}–ZrO_2 catalysts does not affect the mass transfer of products and reactants, since no pore plugging takes place. After calcination of SZH at 620°C, some sintering occurred, the pore volume was reduced by 30 to 40%, but the specific surface was maintained at relatively high values. This result suggests the preservation of a great part of the micropore structure, due to the stabilizing effect of the sulfate ion. The absence of fouling by coke deposits was further confirmed by inspection of the micropore and mesopore regions in the pore distribution plots (not shown).

TABLE 1

Textural Properties at Different Stages of the Catalytic Test

Catalysts	S_g (BET) ($m^2\ g^{-1}$)	V_{pore} ($\mu l\ g^{-1}$)	R_{pore} (Wheeler) (Å)
Fresh, dried at 110°C (SZH)	229.0	373.7	32.64
Calcined in air at 620°C (CSZ)	128.5	230.0	35.80
Coked (3 h time-on-stream)	118.0	225.0	38.40

Note. WHSV = 1.6 h^{-1}, 3 h, pure *n*-C_4.

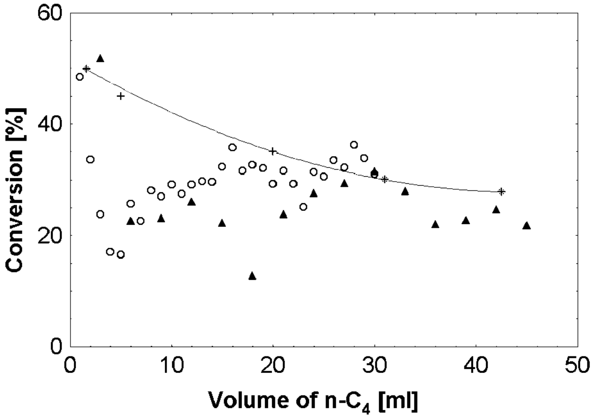

FIG. 1. Activity patterns for small (volume$_{pulse}$/injection period) ratios (0.2 g catalyst, 10 ml/min flow rate): (+) continuous flow, WHSV = 0.8 h^{-1}; (○) 0.5 ml butane/12 min (N_2 carrier); (▲) 3.0 ml/12 min (air carrier).

The XRD spectra (not shown) indicate that the calcined catalysts (CSZ) were mainly tetragonal (T+) with a small amount of monoclinic phase (M−). The ratio of intensities between the main peaks of the two phases $I^T(2\theta = 30.5°)/I^M(2\theta = 28.3°)$ was 1.76. No change detectable by XRD occurred in the crystalline phases upon coking of the catalysts.

Setting conditions for reaction in pulse regime. The mass of catalyst to be used was fixed at 0.2 g and the carrier flow rate at 10 ml/min. A suitable pulse volume and injection period then had to be determined in order to avoid coke "stripping" by the carrier gas in the time intervals between injections. Two different carriers (N_2 and air) were used in order to check whether coke could be eliminated differently depending on the carrier. Stripping occurred when the reactor was directly connected to the chromatographic column and the injection period had to be equal to the time of chromatographic analysis (12 min) (Fig. 1). For these conditions and for 0.5 and 3 ml pulse volume the conversion pattern displayed a big scatter. Almost no coke was detected on these catalysts at the end of the run, indicating that the carrier removed coke precursors between injections. The effect was similar for both the N_2 and the air carriers. Note in Fig. 1 that the original level of conversion was higher than the final stable value although no coke was detected on the catalyst at the end of the run. This suggests that factors other than coking may also be responsible for the decay

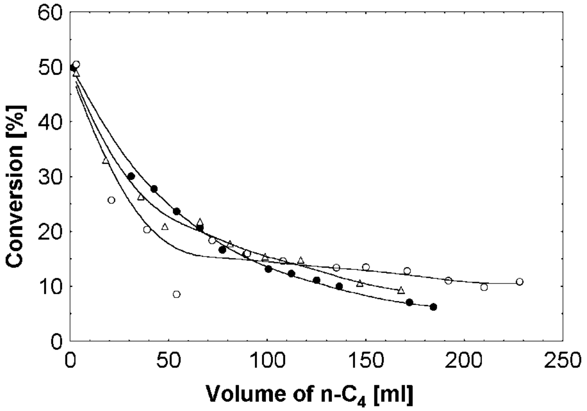

FIG. 2. Comparison between pulse (10 ml/min carrier, 0.2 g catalyst) and continuous flow (0.2 g catalyst, WHSV = 1.6 h^{-1}): (●) continuous flow, pure *n*-butane; (○) pulse flow, air carrier, 3 ml every 3 min; (△) pulse flow, N_2 carrier, 3 ml every 3 min.

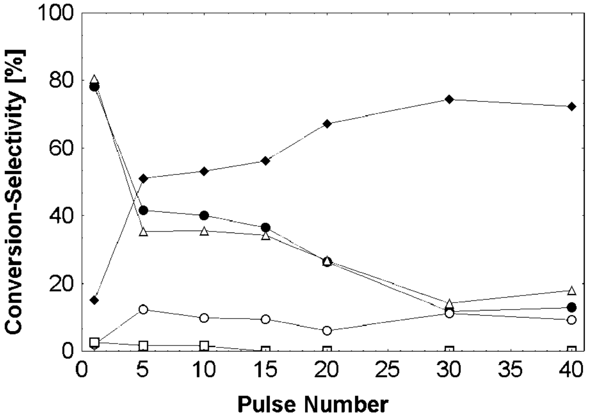

FIG. 3. Conversion and selectivity as a function of pulse number. (●) conversion; (◆) selectivity to *i*-butane; (△) selectivity to propane; (□) selectivity to $C_1 + C_2$ products; (○) selectivity to pentanes (neo-, iso-, and normal).

in conversion, e.g., surface reduction or formation of water that is adsorbed and acts as a poison.

In order to allow a higher (pulse volume/injection period) ratio without increasing the pulse volume too much, the analysis had to be performed off-line by collecting the pulse at the exhaust in a gas-tight ampoule. For an injection rate of about 0.5 ml *n*-C_4 per minute or 3 ml *n*-C_4 every 3 min the conversion plots were stable and similar to the continuous-flow system for any carrier used (Fig. 2). The similar results for N_2 and air seemed to indicate that no chemical interaction with the carrier occurred during coke stripping (e.g., if oxygen traces present in the N_2 carrier could oxidize the coke the effect should be much higher for air). A carrier flow rate of 8–10 ml min^{-1} N_2 and a minimum pulse volume of *n*-C_4 of 0.5 ml were finally adopted. When a single pulse of *n*-C_4 was needed to react over the catalyst, the carrier supply was immediately closed after the pulse left the catalyst bed. For successive pulses, a maximum loop-recharging lag of 1 min was used.

Product analysis. Conversion and selectivity values during isomerization of *n*-C_4 in the pulse mode (0.2 g catalyst, 10 ml/min carrier, 0.5 ml *n*-C_4/pulse) are plotted in Figs. 3 and 4. The conversion was initially very high (almost 80%) but was greatly reduced after a few pulses. Cracking dominated in the initial stage of the reaction and the main product was propane (80% selectivity). At higher values of time-on-stream, cracking decreased sharply and isomerization dominated over other reactions, leading to an increase in the selectivity to *i*-butane which became the main product. The main secondary products were propane and pentanes. All pentanes (neo-, iso-, and normal) were always found, but isopentane was always the most abundant. C_2 products were ethane and ethylene, of which ethane was always the most abundant. The detailed composition of the products at the outlet of the reactor can be seen in Fig. 4 (1° pulse). Traces of butenes and isohexanes (<0.03%) were also detected but accurate determination was not possible.

In the continuous-flow tests, the results were similar, but the measured deactivation seemed less severe, because the first measurement was taken at 5 min time-on-stream when much of the coking process seemed to have already taken place. The measured initial conversion was therefore much lower, 35 to 50% for WHSV values between 0.8 and 2.5 h^{-1}. The decrease in activity was also more rapid in the first minutes of time-on-stream. The major product was *i*-butane obtained at selectivity values of 75 to 90% during most of the reaction. The initial selectivity to propane was moderately high in all cases (10 to 20%), but was reduced to negligible values after 3 h of reaction (<3%).

Selectivity ratios were obtained for an extensive series of runs (continuous flow, WHSV = 0.8 to 2.5 h^{-1}, activation

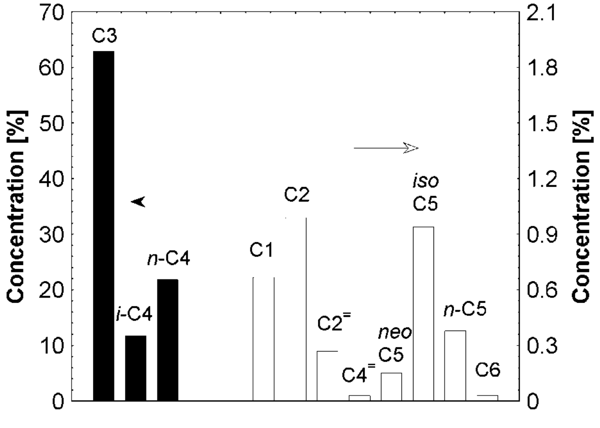

FIG. 4. Composition of the first pulse (0.5 g catalyst, 10 ml/min carrier flow rate, 0.3 ml butane/pulse): C_1, methane; C_2, ethane; C_3, propane; C_4, butanes; C_5, pentanes; C_6, hexanes; $C_2^=$, ethylene; $C_4^=$, butenes (butanes and propane, left ordinate axis; others, right ordinate axis).

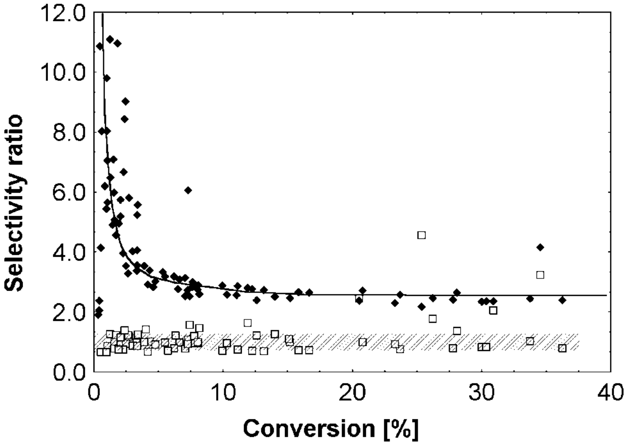

FIG. 5. Selectivity ratios as a function of conversion: (□) propane/pentanes; (◆) iso-pentane/*n*-pentane.

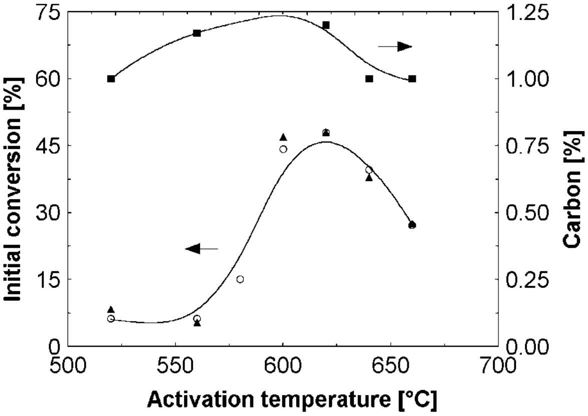

FIG. 6. Coke content (after 2 h reaction) and initial conversion (5 min) as a function of the temperature of calcination (SZH catalyst, continuos flow reaction test, WHSV = 1.0 h^{-1}).

at 620 to 720°C) with different SZ catalysts; they were analyzed as a function of the conversion level. The relationships between *i*-butane, propane, and pentanes were the most well-defined. Methane and ethane displayed apparently no relationship with other products, and the production of light fractions (C_1–C_3) always favored propane. Selectivity to both propane and pentanes in relation to *i*-butane (C_3/*i*-C_4 and C_5/*i*-C_4) decreased with conversion, indicating that the production of propane and pentanes was more affected by deactivation than the isomerization to *i*-C_4.

The most important result was that during most of the reaction, the C_3/C_5 ratio fluctuated in a narrow band around a value of 1.0, indicating that C3 and C5 were mainly formed by dismutation of a C8 oligomeric intermediate (Fig. 5). The presence of scattered points with higher C3/C5 ratios at high values of conversion was addressed to cracking of C5 in the first minutes of the reaction. Of the pentanes, *i*-pentane was the main isomer produced in the molar ratio iso/normal = 2.0 to 3.0 for most of the reaction time. This ratio grew greatly for conversion values lower than 3%. This meant that *i*-pentane was always favored and was almost the only C5 product in conditions of high deactivation.

Dependence of coke content and initial activity on temperature of calcination. The relationship between temperature of activation of the SZH catalysts (initially uncalcined and amorphous), their initial activity, and the amount of coke produced after 3 h of reaction can be seen in Fig. 6. In every case the amount of coke on the fully deactivated catalyst was very small, about 1%. There was a slight increase in the coke content in the 550 to 650°C zone, coinciding with maximum activity in *n*-butane isomerization. However, the variation was not significant (<20%), indicating that the catalyst coking was less sensitive to the activation conditions. At low temperatures (<500°C), no activity was detected and no coke formed on the catalyst, a fact related to the crystallinity of the catalyst: activity is often linked to the appearance of the tetragonal crystalline phase; amorphous catalysts are inactive (6, 10).

If we suppose that for higher initial conversions the total number of gaseous products for a given time increases accordingly, then the reaction pathways leading to *i*-C_4, C_5, and C_4 and those leading to coke seem weakly coupled because the final coke content is nearly always the same. A detailed balance of which carbon atoms go to coke and which to gaseous products, for every pulse, would be needed in order to elucidate this point.

Dependence of coke content and activity on time-on-stream. The relationship between time of reaction, isomerization activity, and coke content in continuous-flow mode is shown in Figs. 7 and 8. Almost all coking occurred within the first 12 min of reaction. The carbon content (area under the TPO curve) did not increase substantially

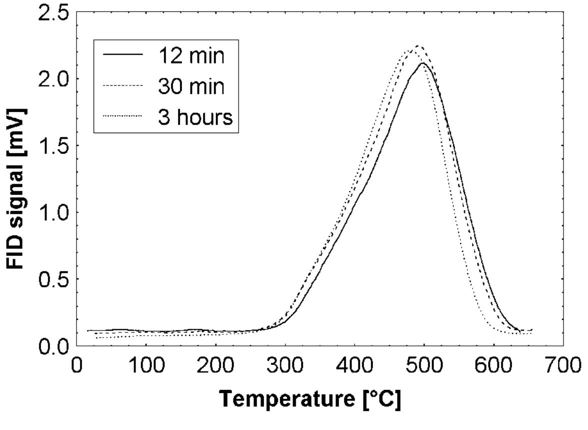

FIG. 7. TPO profiles for CSZ catalysts coked at different values of time-on-stream (WHSV = 1.6 h^{-1}).

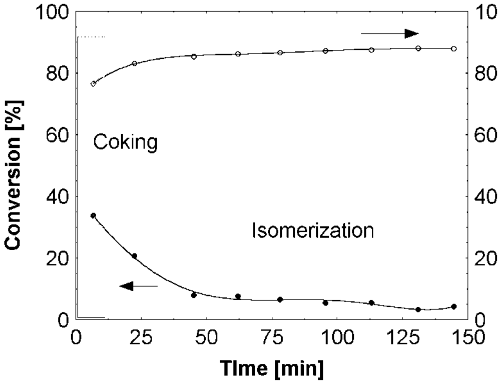

FIG. 8. Span of coking and isomerization reactions (WHSV = 1.6 h^{-1}).

with longer time-on-stream. However, total deactivation required well over 1 h. The deposit was burned with a maximum at 500°C for the three samples. The absence of shifts in the peak maximum may indicate that no changes in the degree of polymerization took place after 12 min time-on-stream.

Coking patterns during the first moments of the reaction were obtained by means of the pulse technique and they were correlated with an exponential expression (not shown). The data could be approximately fitted by an exponential relation $\%C = A \times (1 - \exp(B \times Vol_{n\text{-C4}}))$ with $A = 1$–1.25% (final C content). Voorhies-like expressions $\%C = A \times Vol_{n\text{-C4}}^{B}$ (26) could not reflect the asymptotic pattern of deactivation. Lowering the activation temperature from 620°C (CSZ^{620}, thoroughly dehydrated catalyst) to 300°C (CSZ^{300}, partially hydrated) reduced the activity for isomerization (conversion and selectivity to *i*-butane were both less than 10% throughout the run) but coking was less affected and a limit value of about 1.2% carbon on the catalyst was again obtained.

Coke characterization by TPD/TPO. Coke characterization results can be seen in Fig. 9. As in Fig. 7, the TPO profile showed a maximum at 500°C. Interestingly, stripping with an inert gas at high temperatures was found to remove the coke deposit completely. A subsequent TPO (not shown) confirmed the total removal of the carbon. Even more unusual was that the desorbed products were detected only by methanation; small oxygenated molecules such as CO or CO_2 are typically detected only in this way. Such stripping cannot be related to the adsorption of species on the surface during the activation process because no peak was detected in the case of activated and not coked catalysts (blank, not shown). One possible explanation of these results is that the carbonaceous deposit was oxidized at some redox sites on the catalyst surface and converted into CO and CO_2, which were then after methanation detected by the FID. Related results obtained by Wan *et al.* (27) and Srinivasan *et al.* (28) indicate that sulfated zirconia catalysts can oxidize aromatic compounds to carbon dioxide in an oxygen-free atmosphere. Benzene and pyridine have been found to decompose into CO_2 and coke with the evolution of mainly SO_2 and some O_2. The oxidizing groups have been presumed to be sulfate and lattice oxygen ions.

Coke solubility and weight. The benzene : methanol mixture, which has wide use in the solubilization of coke for reforming catalysts (25), was used as an exploratory test with a standard solvent; this mixture extracted 30% of the coke. Given the short extraction time and the mild conditions used, coke over SO_4^{2-}–ZrO_2 was considered very soluble. The extractions with pure solvents had the additional objective of assessing the functionality of the coke by its solubility in specific solvents.

A categorization obtained by a sequential solvent elution scheme (29) may be used as a guide (Table 2). Solubility in hexane and benzene was practically zero (see Fig. 10). The TPO profile was only slightly augmented due to some solvent adsorption. In methanol, extraction showed a decrease of the 470°C peak, corresponding to the burning of coke. There was also a new peak at 360 to 375°C, probably indicating adsorbed methanol. Extraction with pyridine was

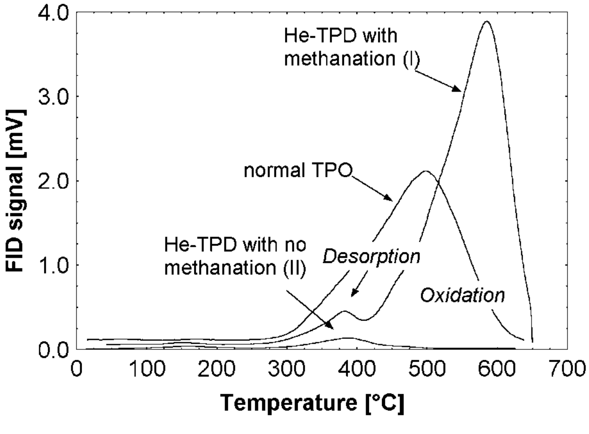

FIG. 9. TPD/TPO profiles of coked catalyst (WHSV = 1.6 h^{-1}, 3 h).

TABLE 2

Coke Functionality and Solvent Affinity

	Solvent or mixture	Eluted compounds
1	Hexane	Saturated hydrocarbons
2	Hexane–benzene (85 : 15)	Aromatic hydrocarbons
3	Chloroform	Polar aromatics, non-basic heterocycles
4	Chloroform–diethyl ether (90 : 10)	Monophenols
5	Diethyl ether–ethanol (97 : 3)	Basic nitrogenated heterocycles
6	Methanol	Highly functional molecules
7	Chloroform–ethanol (97 : 3)	Polyphenols
8	Pyridine–ethanol	Molecules with a high content of N and O

Note. Elution scheme by Alexander and Hasai (29).

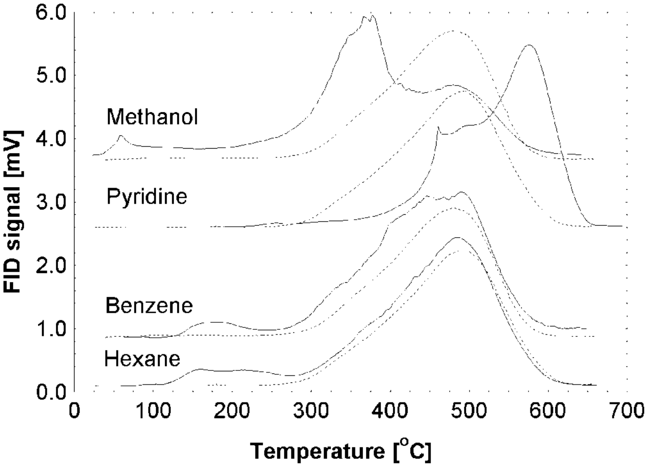

FIG. 10. TPO plots of coked samples before solvent extraction (dotted line) and after solvent extraction (solid line).

thought to be almost complete. The peak corresponding to coke burning almost disappeared and a new peak appeared at 580°C, probably due to pyridine being strongly adsorbed on the acid sites of sulfated zirconia.

In accordance with Table 2, the coke could contain functional groups, e.g., oxygenated ones. Ghençiu and Farcaçiu (30) detected oxygenated products during the reaction of adamantane over sulfated zirconia, which they believed was the result of an oxidation reaction followed by hydride transfers. Another possibility is that cationic carbon fragments are strongly adsorbed due to the presence of highly electronegative sulfate; therefore, neutralization of this effect using basic solvents (pK_b pyridine $>$ pK_b methanol) would be beneficial for removal of the coke.

It is difficult to ascertain whether there was a combination between coke fragments and surface oxygen or S atoms. The only conclusion that can be drawn is that the coke structure is not completely paraffinic. The scarce solubility in benzene cannot be taken as an indication that the coke is not aromatic but that if this were the case, it may be highly polymerized. Solubility of polynuclear aromatic compounds in benzene is scarce (31).

FD-mass. The FD-mass spectrometry results corresponding to the pyridine soluble coke are indicated in Fig. 11. Fragments as heavy as $m/z = 2737$ were recorded. Two maxima, at $m/z = 352$ and $m/z = 532$, were found. These may correspond to heavy polycondensed aromatic fragments of 25 to 40 carbon atoms coming from the parent coke macromolecules. This carbon number can be taken as an estimated lower bound for the carbon number of the average molecule of coke.

ESR results. ESR measurements were made primarily to detect the effect of surface reduction produced by deactivation. Chen *et al.* (32) were not able to detect changes in the oxidation state of Zr in deactivated SZ by use of XPS measurements. This problem was related to the low concentration of these sites. In such cases, a spectroscopic technique with higher sensitivity is needed for the detection of reduced species. ESR seemed a better choice if the reduced species were paramagnetic.

According to some authors, the one-electron oxidation of hydrocarbons on SZ is accompanied by reduction of sulfate to sulfite (33). If strong reduction of sulfate produces SO_2, the electron pair of the sulfate is likely to be allocated to the 3*d* orbitals of Zr, leading to the formation of Zr^{3+} cations. Recently, Vera *et al.* (10) have also argued that anionic vacancies present in the metastable fluoritic structure of SZ may play a crucial role in catalytic activity and that this role is related to oxidizing properties. If vacancies act as electron traps, electron allocation in these defects may produce F^+ centers. Most of the reduced species on the surface of the catalyst and generated upon one electron abstraction

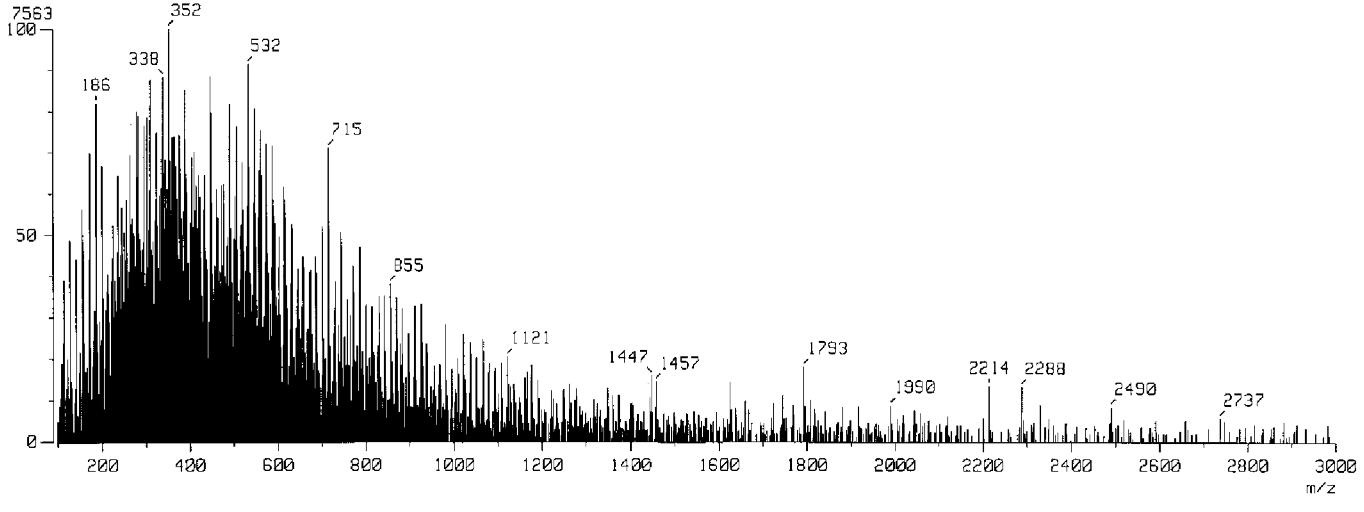

FIG. 11. FD-mass spectrum of the extract obtained by treatment with pyridine.

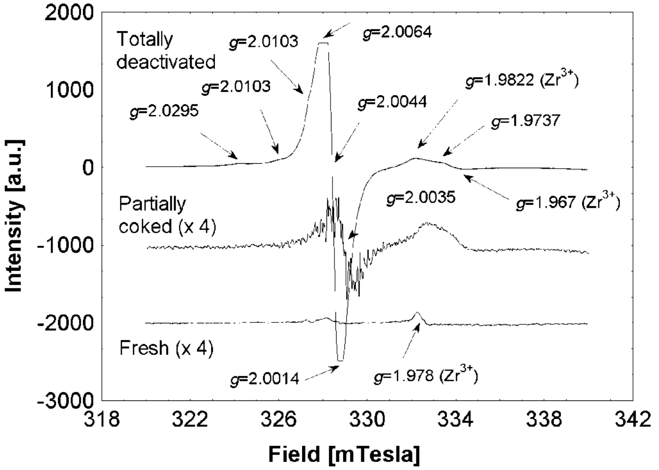

FIG. 12. ESR spectra of fresh, partially coked and completely coked sulfated zirconia. The partially coked sample corresponds to the catalyst coked in reaction with 2 ml of butane. The completely coked sample was deactivated in reaction for 2 h (WHSV = 2.5 h^{-1}).

are paramagnetic and can be distinguished easily from the diamagnetic original one. Zr^{4+} is diamagnetic and Zr^{3+} is paramagnetic. Empty vacancies $V_O^{\bullet\bullet}$ and completely filled vacancies V_O^X are diamagnetic while vacancies with only one electron ($V_O^{\bullet}$) are paramagnetic. Sulfite ion radicals are also paramagnetic and ESR active.

Figure 12 shows the ESR spectra of CSZ before reaction, CSZ partially coked, and CSZ fully deactivated. On the fresh sample the main signal is located at $g = 1.978$ and corresponds to a Zr^{3+} cation. After reacting the sample with butane, the intensity of the Zr^{3+} signal increases and it overlaps with a new one at $g = 1.9737$. Another signal at $g = 1.967$ and also due to Zr^{3+} is more clearly resolved in the case of the coked catalysts. For the fully deactivated sample the intensity of the Zr^{3+} peak at $g = 1.9822$ was about three times that of the fresh catalyst. The new signal at $g = 1.9737$ cannot be assigned to any known paramagnetic species.

A new strong band appeared at $g = 2.0035$–2.0044 on the coked catalysts, with antisymmetric peaks at $g = 2.0064$ and $g = 2.0014$. This new band coincides with that already detected by other researchers on coked sulfated zirconia (12), which was addressed to polyenylic and polyaromatic cations. The new signal is huge and with no hyperfine splittings in the case of the completely deactivated catalyst. The total absence of hyperfine splittings could be related to a high degree of carbonization of the radicals (34). The signal is smaller in the case of the partially coked catalyst and has a wavy profile which may be due to the presence of poorly resolved hyperfine splittings. It must be remarked that the new strong signal occupies the g range where signals due to F^+ centers are expected to be found (35) and it is therefore difficult to say whether ($V_O^{\bullet}$) species were formed or not. A similar strong signal with no hyperfine splittings was detected by Matsuhashi (36) on Pt/SZ after a treatment of reduction with hydrogen. This signal, located at $g = 2.004$, was adressed to F^+ centers. Bobricheva *et al.* (37) in turn have concluded that ESR singlets at $g = 2.002$–2.004 on SZ catalysts should not be addressed to coke or to sulfite ions but to F^+ centers formed during evacuation at high temperature or by reduction during the reaction.

Finally, other small signals at $g = 2.0295$, $g = 2.0181$, and $g = 2.013$ that can be seen in Fig. 12 are likely due to small amounts of adsorbed O_2^- ions.

DISCUSSION

All the experiments tried to draw some valid information about the coking process and its relation to the deactivation of the catalyst. However, main aspects of the results were the little correlation between the coking reaction and the onset and evolution of the activity in isomerization of n-butane, and the small magnitude of coke deposits that had to be made responsible for the activity loss.

The magnitude of the carbonaceous deposit poses some questions about the nature and quantity of the active sites of sulfate-zirconia. The amounts detected were always very small (1.0 to 1.2%) and accompanied a rapid deactivation with no fouling of the porous structure. The surface sulfate content of a catalyst prepared in a standard fashion is about half monolayer (38), and its specific surface area after activation at $T = 600$ to $620°C$ is about 100 to 120 $m^2\ g^{-1}$. For a carbon content of 1% on a coked catalyst, the surface density of carbon, sulfur, and zirconium atoms is therefore as follows: Zr, 8 nm^{-2}; S, 2 nm^{-2}; and C, 4.2 nm^{-2}. The values of Zr and S correspond to a homogeneous distribution (22), while that of C is only an average value.

The coke fragments detected by FD-mass ($m/z = 350$ to 530) may correspond to parent condensed polyaromatic compounds with more than 40 carbon atoms. Carbon in graphitic polycyclic structures has an effective area of 1.8 $Å^2$ (39). Therefore, for a simple bidimensional polyaromatic structure, the packing density of the carbon atoms would be higher than 50 atoms/nm^2. For an agglomerated three-dimensional structure, the density would be even higher. This is many times the average found, 4.2 C/nm^2. This indicates that the coke must be concentrated on only a fraction of the total number of active sites, covering less than 10% of the surface. This also may mean that only a small fraction of the sulfate groups, less than 10%, are active. In this sense, some authors have already posed that only a small fraction of sites may be necessary to carry out the isomerization of n-C_4 onto sulfated zirconia catalysts (11).

Another intriguing point was the occurrence of coking and deactivation on a time scale. The results indicated that coking was mainly confined to the first minutes of reaction (12 min for the continuous flow test of Fig. 8), in coincidence with the stage of low selectivity to *i*-butane, the formation of cracking products, and the initial short-term decrease in conversion. Although coking was completed rapidly, isomerization continued for a relatively long time and the long-term activity decay from 12 min onward, however, was not accompanied by any growth in the carbon deposit and must be addressed to another phenomenon. Our results with SZ corroborate previous ones of Alvarez *et al.* (40) when working with SZ promoted with iron and manganese at reaction temperatures of 100°C. They also reported that although the amount of coke after the first 10 min remained almost unchanged, the activity kept decreasing. From this fact and from the low C/sulfate molar ratio, they suggested that the number of active sites was significantly lower than the total number of sulfate groups or that coke was not the only cause of catalyst deactivation.

With respect to the TPO results, the peak observed in the burning profile (500°C) can be linked to previous results, which indicate that a regeneration performed at 500°C is enough for recovering almost all the original activity of SZ catalysts under *in situ* conditions, while a regeneration at 620°C is needed if, after burning off the carbon deposits, hydration of the catalyst occurs in the presence of humidity (6). The fact that the carbon deposit can be also eliminated by stripping with an inert gas at high temperatures also confirms the fact already reported by some authors that the surface of SZ can oxidize organic adsorbed molecules by reduction of sulfate and loss of lattice oxygen (28).

The results of Fig. 6 describing the influence of the temperature of activation of SZH on the final coke content and the initial conversion of *n*-C_4, and the results of coking on CSZ catalysts either hydrated (CSZ^{300}) or dehydrated (CSZ^{620}), confirmed that coking was much more consistent than isomerization under different hydration conditions. The fact that coke formation seemed to be less affected by the hydration state of the surface than was isomerization was mainly seen in the consistency of the final coke content (1.0 to 1.25% in all cases). Conversely, isomerization activity was much lower in the case of catalysts with higher content of adsorbed water (catalysts activated at $T < 600$ in Fig. 6 or CSZ^{300}). Recalling a bifunctional scheme of reaction depicted in Fig. 13, surface hydration may affect either the dismutation activity or the final hydride transfer. The importance of hydride transfer in the transformation of hydrocarbons on SZ has been studied previously by Iglesia *et al.* (41) who found that addition of hydride transfer agents was beneficial for isomerization while reducing the coking.

If coking cannot be solely and directly addressed as the cause of deactivation then, another phenomenon must be taken into account. Surface reduction seems the most sound choice. For its analysis, we must revise the possible reaction mechanism for both isomerization and coking. There is almost total agreement among researchers that SZ catalysts lack "superacidity" (42, 43) and that the isomerization of *n*-butane proceeds preferentially by a bimolecular route (44, 45). The greater likelihood of a bimolecular reaction path stems from the fact that skeletal rearrangements are more likely to take place in the $C_8H_{17}^+$ intermediate ion than in the carbenium ion *n*-$C_4H_9^+$. If the rearrangements do not involve changes in chain length, the isomerization can proceed by methyl shifts or by formation of protonated cyclopropane intermediates, with intermediate configurations where the charge is placed on the secondary and tertiary carbon atoms. In the case of *n*-$C_4H_9^+$, rearrangement always involves unstable, intermediate primary cations. The bimolecular reaction mechanism requires formation of a C_8 adsorbed intermediate that is first isomerized to a more branched oligomer and finally cracked, releasing isobutane. The C_8 oligomer is commonly posed to be formed by a standard alkylation reaction between an adsorbed carbenium ion and a butene but it has been also suggested that the oligomer is formed by condensation of adsorbed radicals (30, 33). An alkylation-cracking model is depicted schematically in Fig. 13.

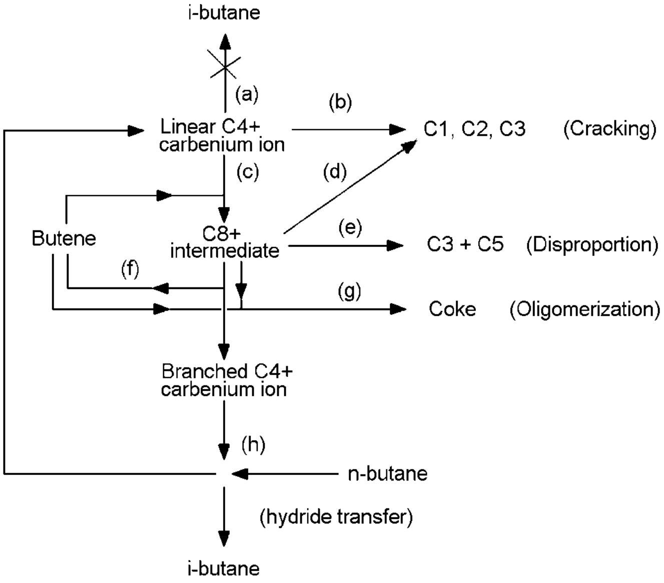

FIG. 13. Hypothetical reaction scheme.

Our results in Fig. 5 provided indirect evidence of the formation of C_8 alkylated intermediates over the catalyst. Propane and pentanes were formed in a ratio near to 1 through a wide range of conversion levels, indicating their common origin from the dismutation of a C_8 species. The results concerning the selectivity ratio between pentanes can also be analyzed on the basis of this mechanism. Pentanes result from the concurrence of three serial reactions: addition of a carbeniem ion (linear or branched) to a butene, rearrangement or the C_8 intermediate, and scission to form propane and pentane. There are more combinations of alkylation, rearrangement by methyl shift, and scission that lead to the formation of *i*-pentane, which is thus statistically favored. Fewer combinations lead to *n*-pentane and neopentane. Isopetane is also thermodynamically favored. The distribution of pentanes in the present study (Fig. 4) is close to the equilibrium composition of pentanes (22). The ratio $i\text{–}C_5/n\text{–}C_5$ increased with decreasing conversion (Fig. 5). A branched C_8-ion intermediate species, produced by addition of a scecondary or tertiary C_4 ion to a butene, requires transformation for the production of *n*-pentane, involving more methyl shifts than for *i*-pentane. Therefore, it seems likely that the increase in deactivation is correlated with a decrease in the ability of the adsorbed oligomers to go throegh methyl shifts and skeletal rearrangements.

Going back to Fig. 13, butenes may come from impurities in the feed as proposed earlier (46), but the bimolecular mechanism seems to take place even if the olefins are thoroughly removed from the feed (47). Butenes have been posed to be formed by oxidative dehydrogenation of butane (10, 27, 47) or by dehydrogenation on Lewis acid–base pairs (48). Ghençiu and Farcaçiu (9) argued that olefins over SZ could be formed by decomposition of previously formed surface sulfite esters. Butenes were indeed detected in small amounts during the reaction (see Fig. 4).

Reducible species on SZ are sulfate ions, Zr^{4+} cations, and nonfilled anionic vacancies. Many mechanisms can be thought to involve these species. In any case, as nonoxidative dehydrogenation is not thermodynamically feasible (10), the final result of the oxidative dehydrogenation will be that oxygen is taken from the surface of SZ in order to remove the excess hydrogen in the form of water:

$$C_4H_{10} + 1/2\, O_{2(\text{catalyst})} \rightarrow C_4H_8 + H_2O\uparrow. \qquad [1]$$

Oxygen loss from the surface likely results in the formation of sulfite ions (Eq. [2]). If reduction proceeds until surface oxygen bound to Zr is lost (Eq. [3]), electrons pairs may transform Zr^{4+} into Zr^{3+}:

$$2\,Zr^{4+} + SO_4^{2-} \rightarrow 2\,Zr^{4+} + SO_3^{2-} + 1/2\,O_2\uparrow \qquad [2]$$

$$\begin{aligned} 2\,Zr^{4+} + SO_3^{2-} &\rightarrow \left(2\,Zr^{4+} + O^{2-}_{\text{surface}}\right) + SO_2\uparrow \\ &\rightarrow (2\,Zr^{4+} + 2\,e^-) + 1/2\,O_2\uparrow \rightarrow 2\,Zr^{3+}. \end{aligned} \qquad [3]$$

An increase in the Zr^{3+} signal was detected in our experiments, while decrease of sulfate and formation of sulfur gaseous species during isomerization of *n*-butane have been previously reported (6, 7). Another source of surface reduction is the formation of carbenium ions, because a net negative charge must be acommodated by the catalyst surface. Again sulfate, Zr cations, and nonfilled anionic vacancies can be thought of as electron acceptors. All of them have been addressed as possible activators of the hydrocarbon molecule. An electron initially withdrawn from the hydrocarbon was thought to be located on the sulfate ion by Farcaçiu *et al.* (30, 33) and on the Zr^{4+} cation by Vera *et al.* (10). The possible role of anionic vacancies for activating the butane molecule and/or hydrogen atoms has also been recently addressed by Matsuhashi (36) (Pt/SZ catalysts in the presence of H_2). Bobricheva *et al.* (37) found that both Zr^{3+} and F^+ ($V_O^\bullet$) centers interact with n-butane and hydrogen but suggested that the first where the key activators. In our ESR experiments, apart from Zr^{3+}, the presence of other paramagnetic reduced species like sulfite ion radicals and ($V_O^\bullet$) could not be detected but cannot be ruled out because the great intensity of the signal at $g = 2.0035\text{–}2.0044$, most likely due to organic radicals, made it difficult to detect other signals. Matsuhashi (36) detected ($V_O^\bullet$) over Pt/SZ in the presence of H_2. Electron trapping seemed to occur due to a transfer from $H^\bullet$ to anionic vacancies. Formation of protonic sites that increase the Brønsted acidity on Pt/SZ has been reported in the past (49).

The above scheme (Eqs. [1]–[3]) implies that the initial dehydrogenation of butane is noncatalytic, since the surface of the catalysts behaves as a reactant. A catalytic cycle can be achieved only if the surface can be reoxidized. However, the presence of oxygen in the reaction medium and at the temperature of reaction has no effect on stability (10), indicating that surface reoxidation can be performed only at high temperatures. A similar reasoning has led some authors to postulate that the fast deactivation of SZ catalysts is due to the availability of multiple pathways: coking by oligomerization of alkenes, coking by coupling of free radicals, and loss of oxidizing ability due to the formation of reduced species (9).

The concurrence of coking, isomerization, and reduction gives more free variables to explain the catalytic chemistry of SZ, which now can be described by a more comprehensive model than the original one containing only acid sites. For the deactivation phenomena found in this work the short-term fast deactivation could be associated to both coking and reduction. Long-term deactivation could be now associated solely to reduction. However, it is apparent that more experimental work is needed to study both effects in detail. Due to their high sensitivity to small amounts of reduced paramagnetic species, it is expected that ESR techniques will be selectively chosen for this purpose. However, the low temperatures (liquid nitrogen) needed for high resolution in ESR seem to hamper any possibility of *in situ* studies.

CONCLUSIONS

—A main conclusion is that long-term deactivation of SZ can not be explained by coking only, which accounts only for the short-term decline in conversion. This result confirms some early reports for Fe, Mn–SZ catalysts (27). Our ESR experiments indicated that surface reduction of the SZ catalyst also occurs and this could be hinted as the additional factor in long-term deactivation. An increase in the population of Zr^{3+} was detected over deactivated catalysts. Surface anionic vacancies could have also acted as electron traps but signals for these species and those due to carbonaceous deposits could not be resolved.

—The coke deposits are almost all produced during the first 5 to 10 min of reaction, when the cracking and formation of olefins are more important. The coke content in totally deactivated catalysts is 1.25% or less. No limitation to mass transfer is posed by this amount of coke.

—The small amount of coke that produces the deactivation and the high molar weight of the fragments as measured by FD-mass indicate that the deactivated sites are only a small fraction of the total.

—The coke deposit can be removed by stripping with an inert gas at sufficiently high temperature. In this case, surface groups are reduced (SO_4^{2-} is thought to be converted into SO_2) and the coke is converted into CO_2 and CO.

—The distribution of products confirmed the existence of a bimolecular mechanism as posed by many authors. The bimolecular path would be preferred because of the lower energy of its intermediates.

—Coking is less affected than is isomerization by the conditions of activation, a fact related to hydration, which seems to prevent the dismutation or hydride transfer steps.

ACKNOWLEDGMENTS

We are grateful to Prof. Hattori (CARET, Hokkaido University, Sapporo, Japan) for useful discussion and to Dr. Sato (CARET) for taking the FD-mass spectrum.

REFERENCES

1. Davis, B. H., Keogh, R. A., and Srinivasan, R., *Catal. Today* **219**, 20 (1994).
2. Song, X., and Sayari, A., *Catal. Rev. Sci. Eng.* **38**, 329 (1996).
3. Yaluris, G., Larson, R. B., Kobe, J. M., Gonzalez, M. R., Fogash, K. B., and Dumesic, J. A., *J. Catal.* **158**, 336 (1996) 336.
4. Sohn, J. R., and Kim, H. W., *J. Mol. Catal.* **52**, 361 (1989).
5. Yori, J. C., Luy, J. C., and Parera, J. M., *Appl. Catal.* **46**, 103 (1989).
6. Comelli, R. A., Vera, C. R., and Parera, J. M., *J. Catal.* **151**, 96 (1995).
7. Ng, F. T. T., and Horvat, N., *Appl. Catal. A: General* **123**, 197 (1995).
8. Xu, B.-Q., and Sächtler, W. M. H., *J. Catal.* **167**, 224 (1997).
9. Ghençiu, A., and Farcaçiu, D., *J. Mol. Catal.* **109**, 273 (1996).
10. Vera, C. R., Yori, J. C., and Parera, J. M., *Appl. Catal. A* **167**, 75 (1998).
11. Yori, J. C., and Parera, J. M., *Appl. Catal. A* **129**, L151 (1995).
12. Spielbauer, D., Mekhemer, G. A. H., Bosch, E., and Knözinger, H., *Catal. Lett.* **36**, 59 (1996).
13. Keogh, R. A., Sparks, D. E., and Davis, B. H., *Stud. Surf. Sci. Catal.* **88**, 647 (1994).
14. Pinna, F., Signoretto, M., Strukul, G., Cerrato, G., and Morterra, C., *Catal. Lett.* **26**, 339 (1994).
15. Hosoi, T., Shimidzu, T., Itoh, S., Baba, S., Takaoka, H., Imai, T., and Yokoyama, N., *in* "Symposium on Preparation and Characterization of Catalysts," Preprints, ACS Petroleum Division, Los Angeles Meeting, September 1988, Vol. 33(4), p. 562, 1988.
16. Sayari, A., and Dicko, A., *J. Catal.* **145**, 561 (1994).
17. Ebitani, K., Konno, H., Tanaka, T., and Hattori, H., *J. Catal.* **143**, 322 (1993).
18. Yori, J. C., D'Amato, M. A., Costa, G., and Parera, J. M., *Latin Am. Appl. Res.* **24**, 257 (1994).
19. Yori, J. C., D'Amato, M. A., Costa, G., and Parera, J. M., *J. Catal.* **153**, 218 (1995).
20. Parera, J. M., *Catal. Today* **15**, 481 (1992).
21. Vera, C. R., and Parera, J. M., *J. Catal.* **165**, 254 (1997).
22. Vera, C. R., Doctoral thesis, Universidad Nacional del Litoral, Santa Fe, Argentina, 1995.
23. Fung, S. C., and Querini, C. A., *J. Catal.* **138**, 240 (1992).
24. Yori, J. C., Luy, J. C., and Parera, J. M., *Catal. Today* **5**, 493 (1989).
25. Parera, J. M., Fígoli, N. S., Beltramini, J. N., Churin, E. J., and Cabrol, R. A., "Proceedings 8th International Congress on Catalysis," Dechema, Verlag-Chemie, Vol. II, 1984.
26. Butt, J. B., "Catalysis, Science and Technology" (J. R. Anderson and M. Boudart, Eds.), Vol. 6. Springer-Verlag, Berlin, 1984.
27. Wan, K. T., Khouw, C. B., and Davis, M. E., *J. Catal.* **158**, 311 (1996).
28. Srinivasan, R., Keogh, R. A., Ghençiu, A., Farcaçiu, D., and Davis, B. H., *J. Catal.* **158**, 502 (1996).
29. Alexander, G., and Hazai, I., *J. Chromatogr.* **217**, 19 (1981).
30. Farcaçiu, D., Ghençiu, A., and Li, J. Q., *J. Catal.* **158**, 116 (1996).
31. Larsen, J. W., Green, T. K., and Kovac, J., *J. Org. Chem.* **50**, 4729 (1985).
32. Chen, F. R., Coudurier, G., Joly, J.-F., and Vedrine, J. C., *J. Catal.* **143**, 616 (1993).
33. Ghençiu, A., and Farcaçiu, D., *Chem. Commun.* **169**, (1996).
34. Retcofsky, H. L., Hough, M. R., Maguire, M. M., and Clarkson, R. B., "Coal Structure" (Martin L. Gorbaty and K. Ouchi, Eds.), Advances in Chemistry Series Vol. 192. Am. Chem. Soc., Washington, DC, 1981.
35. Torralvo, A. J., Alario, M. A., and Soria, J., *J. Catal.* **86**, 473 (1984).
36. Matsuhashi, H., "Proceedings of the 82th Japan Catalysis Conference, Matsuyama, Japan, 16–19 September 1998." Catalysis Society of Japan.
37. Bobricheva, I. V., Stavitsky, I. A., Yermolaev, V. K., Kotsarenko, N. S., Shmachkova, V. P., and Kochubej, D. I., *Catal. Lett.* **56**, 23 (1998).
38. Morterra, C., Cerrato, G., Emanuel, C., and Bolis, V., *J. Catal.* **142**, 349 (1993).
39. Caruso, F., Jablonski, E. L., Grau, J. M., and Parera, J. M., *Appl. Catal.* **51**, 195 (1989).
40. Alvarez, W. E., Liu, H., and Resasco, D. E., *Appl. Catal. A* **162**, 103 (1997).
41. Iglesia, E., Soled, S., and Kramer, G., *J. Catal.* **144**, 238 (1993).
42. Drago, R. S., and Kob, N., *J. Phys. Chem. B* **101**, 3360 (1997).
43. Adeeva, V., de Haan, J. W., Jänchen, J., Lei, G. D., Schünemann, V., van de Ven, L. J. M., Sächtler, W. M. H., and van Santen, R. A., *J.Catal.* **151**, 364 (1995).
44. Adeeva, V., Lei, G. D., and Sächtler, W. M. H., *Catal. Lett.* **33**, 135 (1995).
45. Liu, H., Adeeva, V., Lei, G. D., and Sächtler, W. M. H., *J. Mol. Catal. A* **100**, 35 (1995).
46. Coelho, M. A., Alvarez, W. E., Resasco, D. E., Sikabwe, E. C., and White, R. L., *Catal. Today* **28**, 415 (1996).
47. Tábora, J., and Davis, R. J., *J. Am. Chem. Soc.* **118**, 12240 (1996).
48. Yori, J. C., and Parera, J. M., *Appl. Catal. A* **147**, 145 (1996).
49. Ebitani, K., Tsuji, J., Hattori, H., and Kita, H., *J. Catal.* **135**, 609 (1992).